Journal of Physics: Conference Series **100** (2008) 052053 doi:10.1088/1742-6596/100/5/052053

Stability and geometry of free-standing III-V nanorods

R. Leitsmann and F. Bechstedt

Institut für Festkörpertheorie und -optik, Friedrich-Schiller-Universität, Max-Wien-Platz 1, 07743 Jena, Germany

E-mail: roman@ifto.physik.uni-jena.de

Abstract. We report *ab initio* investigations of hexagon-shaped [111]/[0001] oriented III-V semiconductor nanowires with varying crystal structure, varying surface passivation, and varying diameter. Their stability is dominated by the free surface energies of the corresponding facets which differ only weakly from those of free surfaces. We observe a phase transition between local zinc-blende and wurtzite geometry of the rods versus the preparation conditions of the surfaces, which is accompanied by a change in the facet orientation.

Higly anisotropic needlelike crystals (whiskers) have long been subject of physics and materials science. This interest, especially in the ultimately thin varieties, has been recently stimulated by the potential need as building blocks for nanoscale electronic and photonic devices [1, 2]. The synthesis of nanowires based on a wide range of material systems [3, 4, 5, 6, 7, 8, 9, 10] have been reported. Because of their considerable technological potential, nanowires or nanorods consisting of III-V semiconductors are of special interest. In the most cases the growth direction of III-V semiconductor nanorods is parallel to the [111] axis of the bulk zinc-blende (*zb*) structure, which is the ground-state structure of the common III-V compounds. However, in contrast to bulk crystals the crystal structure of the nanowires may differ noticable, depending on growth conditions and growth method. In particular, changes of the crystal symmetry from the cubic to the hexagonal stacking of the cation-anion bilayers have been observed in many cases [3, 4, 7, 8, 9, 10].

In the present article, we examine free-standing, hexagon-shaped InAs nanowires with varying surface facet orientation and passivation, several diameters, and two crystal structures close to the thermal equilibrium. The results are extrapolated to the case of extremely thick rods with almost bulklike surfaces. The favored geometries are studied versus the preparation conditions of the wires.

The total-energy (TE) calculations are performed in the framework of the density functional theory (DFT) and the local density approximation (LDA) as implemented in the Vienna *ab initio* simulation package (VASP) [11]. The outermost *s*-, *p*-, and (in the case of In) *d*-electrons are treated as valence electrons whose interaction with the remaining ions is modeled by pseudopotentials generated within the projector-augmented wave (PAW) method [12]. The energy cutoff of the plane-wave basis is tested to be sufficient with 15 Ry. The Brillouin-zone summations are restricted to M$\times$N$\times$2 meshes of special points according to Monkhorst and Pack [13] with M=N=5 for diameters smaller than 1 nm and M=N=3 for diameters larger than 1 nm. For zinc blende the minimization of the total energy leads to a theoretical cubic lattice constant $a_0 = 6.03$ Å as well as to a negative cohesive energy per InAs pair (without spin-polarisation corrections) $\mu_{InAs}^{\mathrm{bulk}} = -8.88$ eV. Free surfaces of *zb* or wurtzite (*w*) crystals are studied within the repeated-slab method using material slabs of about 14 to 17 Å separated by a vacuum region of the same thickness [14]. We consider only rods and lateral unit cells with hexagonal cross-sections, so that the point-group symmetry C_{3v} is conserved for arrangements of both *zb*- and *w*-structure rods.

Neighboring rods are separated by a vacuum region of about 2 nm, which was tested to be sufficient for converged calculations. In addition to the two different stackings (*zb* or *w*) of the bilayers in growth direction, two different types I and II of surface facets are studied (see Fig. 1). Type-I wires contain $\{11\bar{2}\}$ or $\{1\bar{1}00\}$ side facets in the *zb* or *w* case, respectively. In the type-II case, $\{110\}$ facets for *zb* and $\{1120\}$ facets for *w* occur. The construction of the atomic structures in Fig. 1 starts from a cation-anion bond parallel to the growth directions. The nearest-neighbor atoms occur at the corners of a tetrahedron along cubic body diagonals. In the wurtzite case each second tetrahedron in stacking direction is twisted by 180° resulting in a shortening of the period of translational symmetry in [0001] growth direction.

The side facets of the two wire types considered are stoichiometric and electrostatically neutral. Even the numbers of cation and anion dangling bonds (DBs) are equal in each irreducible slab. To simulate a possible passivation of the DBs at the wire surfaces due to absorption of environmental atoms or metal atom excess, we use fractionally charged pseudohydrogen with a valence charge $Z = 0.75$ (H^*) or 1.25 (H^{**}) [15]. Figure 1 indicates remarkably different geometries of the two types of side facets. In the type-II case the side facets have only one DB per surface atom and exhibit rather similar geometries. In contrast, type-I side facets differ in their bonding structures. In the average, each surface atom possesses 4/3 (*zb*) or 3/2 (*w*) DBs. However, already for *zb* stacking their distribution depends on the orientation of a $\{11\bar{2}\}$ facet. Neighboring facets, for instance $(1\bar{1}2)$ and $(\bar{2}11)$, are different with respect to their DB distribution. The atoms in the uppermost atomic layer possess two DBs for *zb*-crystal structures and an averaged value of 1.5 DBs for *w*-crystal structures. However, the atoms in the second atomic layer of the $(11\bar{2})$*zb* surface exhibit one additional dangling bond. In principle, the situation is somewhat more complicated because of the existence of edges which modify the picture of free surfaces for finite wire sizes. However, for thick rods, i.e., in the limit of large diameters, the facets represent free surfaces.

In order to study the fact that in a rod not all In and As atoms are fourfold coordinated but the cation and anion DBs occur pairwise, we investigate the formation energy [14] of a rod with a certain surface area consisting of symmetry-equivalent facets defined by diameter D and length L

$$\begin{aligned} E_{\rm surf}^{\rm rod} &= E_{\rm tot}^{\rm rod}(N_{InAs}, N_{\rm mol}) - N_{InAs}\mu_{InAs}^{\rm bulk} \\ &- N_{\rm mol}\mu_{H^*-H^{**}}^{\rm mol} - N_{\rm mol}\Delta\mu_{H^*-H^{**}}, \end{aligned} \quad (1)$$

where $E_{\rm tot}^{\rm rod}(N_{InAs}, N_{\rm mol})$ is the total energy of a rod containing N_{InAs} cation-anion pairs with DBs or passivated by $N_{\rm mol}$ pairs of pseudohydrogens H^* and H^{**}. This energy is related to the corresponding bulk energy $N_{InAs}\mu_{InAs}^{\rm bulk}$ and to the energy of the $N_{\rm mol}$ $H^* - H^{**}$ molecules used to passivate the total number of $2N_{\rm mol}$ DBs. We assume that the rods are in thermodynamic equilibrium with a bulk *zb* InAs crystal that represents a reservoir for In and As atoms. The passivation is governed by a reservoir of $H^* - H^{**}$ molecules with the chemical potential $\mu_{H^*-H^{**}}$. The variation of this chemical potential allows to model the environmental influence during the growth process [16]. Here $\mu_{H^*-H^{**}}^{\rm mol}$ (calculated as the negative binding energy) corresponds to the situation where the rod surface is exposed to molecular pseudohydrogen at vanishing temperature. However, due to the need to overcome the dissociation barrier, the stable passivated surface structures will not form immediately. Practically no pseudohydrogen is present on the clean surface. The temperature and pressure dependence $\Delta\mu_{H^*-H^{**}}$ of $\mu_{H^*-H^{**}}$ can be approximated similarly to that of a two-atomic ideal gas. A slightly negative potential (e.g. $\Delta\mu_{H^*-H^{**}} \approx -1$ eV) may model typical MOVPE growth conditions while fully passivated surfaces may form for $\Delta\mu_{H^*-H^{**}} > 0$ where atomic pseudohydrogen is available.

The formation energy (1) depends on the geometry (diameter D, length L) of the considered rod and the preparation conditions, i.e., $\Delta\mu_{H^*-H^{**}}$. For a more precise discussion we refer this energy to the surface area $A_{\rm rod} = 2\sqrt{3}\,DL$ of the considered rod and set $\Delta\mu_{H^*-H^{**}} \equiv 0$. The resulting surface free energy per unit area $\tilde{\gamma}(D)$ is also influenced by the energetics of the inner rod atoms and the energetics of the edges between two facets [17, 18]. For $D \to \infty$ the rod surface energy $\tilde{\gamma}(D)$ converges against the surface energy $\tilde{\gamma} = \tilde{\gamma}(\infty)$ of a unrelaxed surface with the considered orientation as demonstrated in Table I. This convergence is faster for passivated rods than for rods with clean facets. For the *w*-crystal structure $\tilde{\gamma}(\infty)$ is not exactly equal to the free surface energy. It contains contributions resulting from the crystal

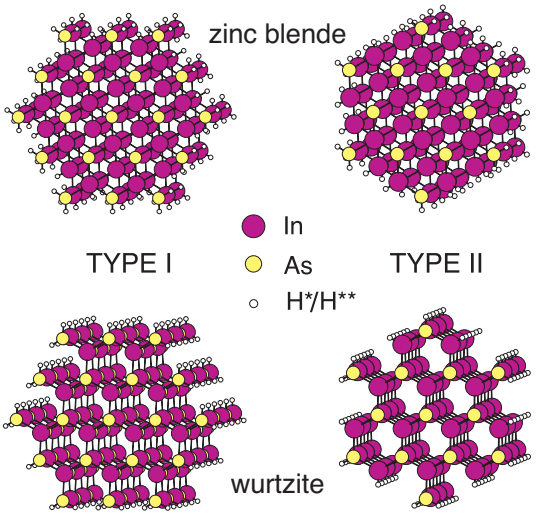

Figure 1. (Color online) Perspective stick and ball representation of type-I and type-II nanowire models with indicated side-facet orientations.

structure change. However, those contributions are very small, $\mu^{\rm bulk}_{InAs}(zb) - \mu^{\rm bulk}_{InAs}(w) \approx 25$ meV, and can therefore be neglected (at least for the considered numbers N_{InAs}). Our surface results are in agreement with other first principles calculations. For instance the free surface energy of the relaxed cleavage (110) surface of InAs with the value of 40.5 meV/Å^2 agrees well with the result of Ref. [18]. Table I exhibits three clear trends. First, the surface energies of the rods are only slightly larger than the one of the corresponding free surface. With rising rod diameter a rapid convergence to the free surface values is observed. The diameter of the rod is of little influence on the stability of the rod, taking as measure the minimum surface energy with respect to the surface area $A_{\rm rod}$ for given volume [19]. Second, for the assumed preparation conditions, $\Delta\mu_{H^*-H^{**}} = 0$, the energies of the passivated surfaces are slightly smaller, indicating the stability of the passivated rods versus such with clean surfaces. Third, the type-I rods with a higher dangling-bond density of the surface possess a larger surfaces energy. Which stacking, *zb* or *w*, in the rod is more stable depends on the passivation and the wire type.

D	Type I		D	Type II	
(Å)	*zb*	*w*	(Å)	*zb*	*w*
7.4	95	110	8.5	85	73
	31	37		28	27
14.8	87	97	12.8	79	81
	29	34		26	28
∞	82	85	∞	65	63
	28	34		23	25

Table 1. Surface energies $\tilde{\gamma}(D)$ (in meV/Å^2) for InAs rods of type I or II for varying diameter. The values for large diameters ($D = \infty$) are calculated for free surfaces using the repeated-slab method. The first (second) value has been obtained for clean (passivated) nanorods.

The stability of InAs rods with different stacking, surface orientation, and surface passivation as a function of the preparation conditions is demonstrated by the phase diagram in Fig. 2. We have plotted the surface energy $\gamma(D) = E^{\rm rod}_{\rm surf}/A_{\rm rod}$ according to expression (1) versus the variation of the chemical potential of the passivating species. Because of the weak diameter dependence of the energies we interpolate the values in Table I to rods with a realistic diameter of about 5 nm. One observes a strong influence of the preparation on the rod stability. If mainly passivating molecules of a not too high density are present (yellow region in Fig. 2), the rods prefer clean surfaces of type II with low dangling-bond density, i.e., $\{\bar{1}10\}/\{\bar{2}110\}$ facets. In the presence of dissociated molecules (free radicals H* and H**), i.e., $\Delta\mu_{H^*-H^{**}} > 1$ eV (blue region in Fig. 2), the rod should be passivated and possesses type-I facets, i.e., those with originally higher dangling-bond densities. In this case, a clear favorization of the wurtzite

stacking versus the zinc-blende stacking can be stated. However, in all other cases the energies of the two different bilayer stackings are very close in energy, so that probably other (e.g. kinetic) aspects of the rod growth are more important for a given stacking than energies derived for pure equilibrium situations. Under intermediate conditions, i.e., $\Delta\mu_{H^*-H^{**}}$ between -1 eV and 1 eV (green region in Fig. 2), passivated type-II facets are preferred. The experimental results concerning InAs are usually not unique. However, there is one report on *zb* nanorods with probably $\{\bar{1}10\}$ facets [6] where the wires have been grown by a laser-assisted catalytic growth technique.

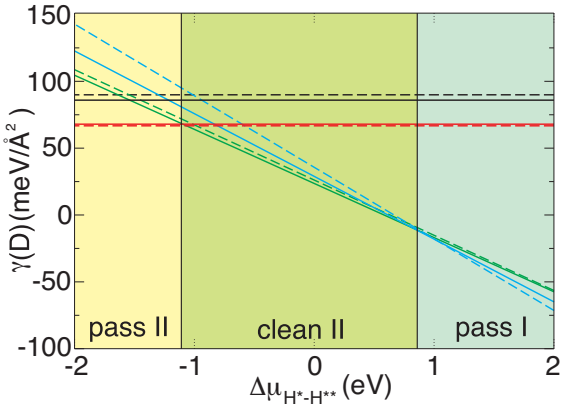

Figure 2. (Color online) Surface energy per surface area $\gamma(D)$ of InAs rods in zinc-blende (solid line) and wurtzite (dashed line) structure with a thickness of about 5 nm versus the variation of the chemical potential $\Delta\mu_{H^*-H^{**}}$ of the passivating molecules. Clean and passivated type-I rods are shown in black and blue, while clean and passivated type-II rods are shown in red and green. The three different stability regions are indicated.

In conclusions, we have shown that the rod energetics near the thermodynamic equilibrium are ruled by their surfaces. The formation energies of those rods approach the energies of the corresponding free surfaces. The orientation for the surface facets and the passivation of their dangling bonds play an important role, in contrast to the bilayer stacking in growth direction. Our studies are able to explain the wide variety of results concerning facet orientation and bilayer stacking found for InAs rods.

Acknowledgments

We gratefully acknowledge valuable discussions with B. Mandl and G. Bauer from the University of Linz. Financial support was provided by the Fonds zur Förderung der Wissenschaftlichen Forschung (Austria) via SFB25 IR-ON and the EU NoE NANOQUANTA (Project No. NMP4-CT-2004-500198). We thank the Höchstleistungsrechenzentrum Stuttgart for granted computer time.

References

[1] D. Appell, Nature (London) **419**, 553 (2002).
[2] J. Wang, M.S. Gudiksen, X. Duan, Y. Cui, and C.M. Lieber, Science **293**, 1455 (2001).
[3] K. Hiruma, M. Yazawa, K. Haraguchi, and K. Ogawa, J. Appl. Phys. **74**, 3162 (1993).
[4] K. Hiruma, M. Yazawa, T. Katsuyama, K. Ogawa, K. Haraguchi, and M. Koguchi, Appl. Phys. Rev. **77**, 447 (1995).
[5] X. Duan, J. Wang, and C.M. Lieber, Appl. Phys. Lett. **76**, 1116 (2000).
[6] X. Duan and C.M. Lieber, Adv. Mater. **76**, 1116 (2000).
[7] B.J. Ohlsson, M.T. Björk, M.H. Magnusson, K. Deppert, and L. Samuelson, Appl. Phys. Lett. **79**, 3335 (2001).
[8] M.T. Björk, A. Fuhrer, A.E. Hansen, M.W. Larsson, L.E. Froberg, and L. Samuelson, Phys. Rev. B **72**, 201307 (2005).
[9] M.T. Björk, B.J. Ohlsson, T. Sass, A.I. Persson, C. Thelander, and M.H. Magnusson, Appl. Phys. Lett. **80**, 1058 (2002).
[10] P. Mohan, J. Motohisa, and T. Fukui, Nanotech. **12**, 298 (2005)
[11] G. Kresse and J. Furthmüller, Comp. Mat. Sci. **6**, 15 (1996); Phys. Rev. B **54**, 11169 (1996).
[12] G. Kresse and D. Joubert, Phys. Rev. B **59**, 1758 (1998).
[13] M.J. Monkhorst and J.D. Pack, Phys. Rev. B **13**, 5188 (19976).
[14] F. Bechstedt, *Principles of Surface Physics* (Springer 2003).
[15] K. Shiraishi, J. Phys. Soc. Jpn. **59**, 3455 (1990).
[16] W.G. Schmidt, P.H. Hahn, F. Bechstedt, N. Esser, P. Vogt, A. Wange, and W. Richter, Phys. Rev. Lett. **90**, 126101 (2003).
[17] A. Stekolnikov, J. Furthmüller, and F. Bechstedt, Phys. Rev. B **65**, 115318 (2002).
[18] E. Pehlke, N. Moll, A. Kley, and M. Scheffler, Appl. Phys. A **62**, 525 (1997).
[19] C. Herring, Phys. Rev. **82**, 87 (1951).